Electronic Journal of Biotechnology 77 (2025) 24–34

Contents lists available at ScienceDirect

Electronic Journal of Biotechnology

journal homepage: www.elsevier.com/locate/ejbt

Research article

Improved resistance to basal rot disease and promotion of onion plant growth by *Aspergillus terreus*-mediated silver nanoparticles ☆

Mohamed G.A. Hegazy [a], Mahmoud Gad [b], Sobhi F. Lamlom [c], Islam I. Teiba [d], Osama A.M. Al-Bedak [e,f,*], Muhammad Moaaz Ali [g,h], Eman Alhomaidi [i], Mona Saleh Al Tami [j], Ahmed F. Yousef [k,l], Waleed M. Ali [k]

[a] *Department of Agricultural Botany (Plant Pathology), College of Agriculture, Al-Azhar University, Assiut, Egypt*
[b] *Department of Botany and Microbiology, Faculty of Science, Al-Azhar University, Assiut, Egypt*
[c] *Department of Plant Production, College of Agriculture (Saba Basha), Alexandria University, Alexandria, Egypt*
[d] *Microbiology, Botany Department, Faculty of Agriculture, Tanta University, Tanta, Egypt*
[e] *Assiut University Mycological Centre, Assiut, Egypt*
[f] *ERU Science & Innovation Center of Excellence, Egyptian Russian University, Badr city, Egypt*
[g] *College of Horticulture, Fujian Agricultural and Forestry University, Fuzhou, China*
[h] *State Key Laboratory of Ecological Pest Control for Fujian and Taiwan Crops, College of Plant Protection, Fujian Agriculture and Forestry University, Fuzhou, China*
[i] *Department of Biology, College of Science, Princess Nourah bint Abdulrahman University, Riyadh, Saudi Arabia*
[j] *Department of Biology, College of Science, Qassim University, Saudia Arabia*
[k] *Department of Horticulture, College of Agriculture, University of Al-Azhar, Assiut, Egypt*
[l] *National Key Laboratory for Germplasm Innovation & Utilization of Horticultural Crops, Zhengzhou Fruit Research Institute, Chinese Academy of Agricultural Sciences, Zhengzhou, Henan, China*

GRAPHICAL ABSTRACT

Improved resistance to basal rot disease and promotion of onion plant growth by *Aspergillus terreus*-mediated silver nanoparticles

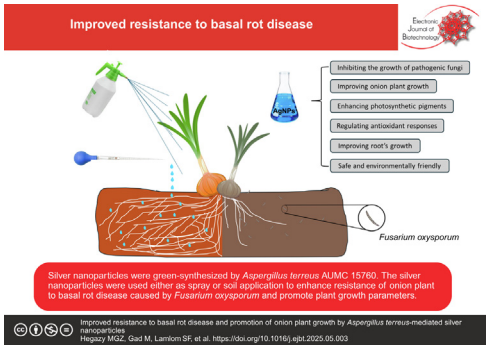

ARTICLE INFO

Article history:
Received 29 January 2025
Accepted 12 May 2025
Available online 24 July 2025

ABSTRACT

Background: Onions, a vital agricultural crop rich in carbohydrates and essential minerals, face severe threats from *Fusarium oxysporum*, the causative agent of basal rot disease. This study assessed the effectiveness of extracellular, green-synthesized silver nanoparticles (AgNPs), produced by *Aspergillus terreus* AUMC 15760, in managing basal rot disease caused by *F. oxysporum* AUMC 15798.

☆ Audio abstract available in Supplementary material.

Peer review under responsibility of Pontificia Universidad Católica de Valparaíso.

* Corresponding author.
E-mail address: osamaalbedak@aun.edu.eg (O.A.M. Al-Bedak).

https://doi.org/10.1016/j.ejbt.2025.05.003

Keywords:
Allium cepa
Antifungal activity
Antioxidant activity
Aspergillus terreus-mediated
Disease management
Ecofriendly fungicides
Greenhouse
Nanotechnology
Onion plant growth promotion
Rot disease resistance
Silver nanoparticles

Results: AgNPs ranging from 12.1 to 28.7 nm were incorporated into PDA media at concentrations of 50, 100, 150, and 200 ppm, achieving fungal growth inhibition rates of 24.88%, 40.77%, 54.44%, and 69.33%, respectively. A greenhouse experiment was carried out using onion seedlings, with a randomized complete block design (RCBD) to compare eight different treatments: 100 ppm AgNPs (spray), 50 ppm AgNPs (spray), 100 ppm AgNPs (soil application), 50 ppm AgNPs (soil application), Dovex spray (50%), Dovex soil application (50%), a negative control, and a positive control. Greenhouse results showed a significant reduction in disease severity, with Dovex lowering it to 20%. AgNPs at 50 ppm reduced severity to 57.77% (soil) and 35.55% (spray), while 100 ppm further decreased it to 31.1% (soil) and 22.2% (spray). The application of 100 ppm AgNPs improved plant growth parameters. It also enhanced chlorophyll *a*, chlorophyll *b*, and carotenoid levels. The greatest reductions in phenolic (0.34 mg/g) and anthocyanin contents (0.48 mg/g), as well as peroxidase (0.44 μmol/min) and catalase activities (0.19 μmol/min), were recorded in plants treated with 100 ppm AgNPs (spray).
Conclusions: AgNPs effectively control basal rot disease, boost plant growth, and regulate antioxidant activity.
How to cite: Hegazy MG, Gad M, Lamlom SF, et al. Improved resistance to basal rot disease and promotion of onion plant growth by *Aspergillus terreus*-mediated silver nanoparticles. Electron J Biotechnol 2025;77. https://doi.org/10.1016/j.ejbt.2025.05.003.

1. Introduction

The onion (*Allium cepa* L.) is a globally cultivated bulb crop known for its high carbohydrate content and valuable micronutrients such as calcium, phosphorus, protein, and vitamin C [1,2]. However, its production is severely threatened by *Fusarium oxysporum* f. sp. *cepae*, the causal agent of basal rot disease, which penetrates the bulb base and storage scales, leading to significant post-harvest losses [3]. This pathogen also affects other *Allium* species, including garlic and shallots [4]. Conventional control strategies—such as crop rotation, resistant cultivars, and synthetic fungicides—have shown limited success and raise environmental and health concerns [5].

Recent advances in nanotechnology have highlighted the potential of silver nanoparticles (AgNPs) as sustainable alternatives to conventional antifungal agents. AgNPs exhibit broad-spectrum antimicrobial activity, offering an effective strategy to reduce reliance on hazardous chemical fungicides [6,7,8]. However, traditional chemical and physical synthesis methods for AgNPs often involve toxic reducing agents, high energy consumption, and environmental concerns [9]. To address these limitations, biological synthesis using microorganisms -particularly fungi- has emerged as an eco-friendly, cost-effective, and scalable approach [10,11,12]. Fungal-mediated synthesis leverages natural biomolecules to stabilize AgNPs, enhancing their biocompatibility and applicability in agriculture [13,14,15,16,17]. For instance, studies have demonstrated the efficacy of fungal-derived AgNPs against phytopathogens like *F. oxysporum* and *Botrytis cinerea*, achieving inhibition rates exceeding 70% while minimizing ecological harm [16,17]. Beyond their antimicrobial properties, AgNPs have transformative applications in agriculture, serving as nanofertilizers, smart delivery systems for pesticides, and catalytic agents for nutrient uptake [18,19,20]. Their dual role in disease suppression and plant growth promotion positions them as a cornerstone of next-generation sustainable farming practices.

Therefore, this study aimed to investigate the antifungal efficacy and growth-promoting effects of biologically synthesized silver nanoparticles (AgNPs) produced by *Aspergillus terreus* AUMC 15760 against *F. oxysporum* AUMC 15798, the causative agent of basal rot in onions. We hypothesized that AgNPs would not only suppress the pathogen effectively but also enhance plant physiological traits under greenhouse conditions. Despite growing interest in nanotechnology for plant disease management, there remains a significant gap in understanding the *in vivo* impact of fungal-mediated AgNPs on both disease suppression and onion plant growth, particularly under pathogen stress. This study addresses that gap by combining antifungal assays with greenhouse trials, offering an eco-friendly alternative to conventional fungicides.

2. Materials and methods

2.1. Fungal strains

From diseased onion bulbs exhibiting indications of basal rot disease, *F. oxysporum* was isolated and identified from certain recently reclaimed sites in Sohag Governorate, Egypt. The disease severity of the *F. oxysporum* strain AUMC 15798 was found to be 88.88 ± 19.25 [21]. As a result, we decided to use environmentally friendly silver nanoparticle synthesis to control this strain in this investigation. This study also exploited a wild strain of *Aspergillus terreus* AUMC 15760 [22] to produce silver nanoparticles in an environmentally safe manner for use in control experiments involving the severity of disease caused by the *F. oxysporum* strain. Both *F. oxysporum* AUMC 15798 and *A. terreus* AUMC 15760 strains were maintained on potato dextrose agar and malt extract agar slants, respectively, at 4°C [23]. The mycelia were also stored at −86°C and lyophilized spores, as well as on cotton balls [24], in the culture collection of the Assiut University Mycological Centre, Assiut Governorate, Egypt.

2.2. Biological synthesis of silver nanoparticles (AgNPs) by A. terreus AUMC 15760

Following the methods of Hamad [25], *A. terreus* AUMC 15760 was grown in 500 mL Erlenmeyer flasks with 100 mL of potato dextrose broth in each flask for seven days at 25°C and 150 rpm. The cell-free supernatant was obtained by centrifugation (10,000 rpm for 10 min at 4°C). A 100 mM $AgNO_3$ solution was mixed with the cell-free supernatant of *A. terreus* AUMC 15760 in 500 mL Erlenmeyer flasks to produce concentrations of 10, 20, 30, 40, and 50% (v/v). The flasks were then incubated at 25°C and 150 rpm until the color of the solution changed. Visual inspection of the solution was regularly used to track the reduction of silver ions to silver nanoparticles.

2.3. Transmission electron microscopy (TEM) characterization of the AgNPs

A 10-fold diluted sample of the produced AgNPs was placed on carbon-coated copper grids and kept under vacuum overnight before being inserted into the sample holder for transmission electron microscopy (TEM) measurements [26]. Using a JEM100CX11 instrument operating at 100 kV (0.23 nm resolution), the size of the AgNPs was ascertained at the Electron Microscopy Unit of Assiut University, Assiut, Egypt.

2.4. In vitro effect of AgNPs on the growth of f. oxysporum AUMC 15798

The impact of the AgNPs on *F. oxysporum* AUMC 15798 was evaluated [27]. Mycelial discs (5 mm in diameter) obtained from a 7-d-old culture of *F. oxysporum* were placed in the center of PDA plates containing AgNPs at 50, 100, 150, and 200 ppm. After 4 d of incubation at 25 ± 2°C, the percentage of inhibition of radial colony growth was calculated. As a negative control, sterilized distilled water was administered to the PDA rather than the AgNP. The percentage of the pathogens' mycelial growth inhibition was calculated according to **Equation 1.**

$$\%\,Inhibition = \frac{(D1 - D2)}{D1} \times 100 \quad (1)$$

where $D1$ = the colony diameter in the control plate and $D2$ = the colony diameter in the treated plate.

2.5. Inoculum preparation

Pathogenicity tests were conducted on 60-d-old onion seedlings (Cultivar: Giza Sabeeni) in a greenhouse at the Department of Plant Pathology, Faculty of Agriculture, Assiut University, Egypt, during the growing season of 2022–2023. Using a barley and sand mixture (1:1) in 500 mL Erlenmeyer flasks, *F. oxysporum* AUMC 15798 was cultured and incubated for 21 d at 25°C to prepare the inoculum. Following the complete filling of the barley sand by *Fusarium* growth, one gram of fungal growth mixture was suspended in ten millilitres of distilled water and vortexed for one minute. Centrifugation (3000 rpm for 5 min at 4°C) was then used to isolate the supernatant containing the *Fusarium* spores. Seven days before the seedlings were planted, the *Fusarium* growth was mixed with sterilized soil at a rate of 3% (w/w) to obtain 1.5×10^4 spores/g soil. Four groups of 25-cm plastic pots were used, one of which was used as a negative control. Before the five onion seedlings were planted, 3 kg of presterilized sand:clay soil (1:2) was placed into each pot.

2.6. Greenhouse experiment

This study was carried out in the experimental greenhouse of the Faculty of Agriculture at Assiut University, Assiut, Egypt. For 7 d, a 5.0% formalin solution was used to sterilize the clay loam soil utilized in the greenhouse experiments [28,29]. The soil was mixed well and covered with a plastic sheet for one week, after which the sheet was removed for an additional week to allow the formalin to completely evaporate. Plastic pots measuring 25 cm in diameter were submerged in a 5.0% formalin solution for 15 min to guarantee sterility. The pots were then left for a few days to eliminate the toxic effects of formalin. As previously indicated, the percentage of disease severity for each treatment was noted at the end of the experiment. Five isolates were used with respect to the fungal pathogen *F. oxysporum*, with each strain being allocated to three pots. Appropriate amounts of water were added to the pots on the basis of the rooting medium moisture level to ensure that the plants were moist. One week after transplanting, the plants were subjected to a water-soluble fertilizer routine. "N20: P20: K20 + TE" compound fertilizers from Green House Egypt Co., Egypt, and "Stimufol Amino compound fertilizers" (which include "25% N, 16% P, 12% K, 2% amino acids, 0.044% boron, 0.17% iron, 0.001% molybdenum, 0.03% zinc, 0.085% copper, 0.01% cobalt, 0.02% magnesium, 0.085% manganese, and EDTA") from Shoura Co., Egypt, were the fertilizers included in this experiment. After 120 d, the percentage of disease severity for each treatment was noted at the end of the experiment. The percentage of disease severity in each treatment was noted, and the basal rot disease grading scale [21] was as follows:

1 = Symptom-free.
2 = Up to 10% rotted roots.
3 = 10–30% rotted roots with up to 10% rotted basal plates.
4 = 100% rotted roots and 10–30% rotted basal plates.
5 = 100% rotted roots and more than 30% rotted basal plates.

2.7. Experimental treatments

The study was executed via a randomized complete block design [30,31]. The experimental treatments included the following: T1 = 100 ppm AgNPs (spray); T2 = 50 ppm AgNPs (spray); T3 = 100 ppm AgNPs (soil application); T4 = 50 ppm AgNPs (soil application); T5 = Spray of Dovex (50%); T6 = Soil application of Dovex (50%); T7 = negative control; and T8 = positive control. In addition, 50% Dovex (azoxystrobin 20% + tebuconazole 30%) was used at a rate of 25 cm^3/100 L as a reference for comparison [21,32].

2.8. Determination of the agronomic parameters

After 120 d from the initial seedling planting [28,29,33], an assessment of the growth parameters was conducted. The shoot and root lengths were measured (in cm) from the base of the bulb to the tip of the plant. Digital calipers were used to measure the bulb and neck diameters (in mm). With a sensitivity of 0.001 g, precision electronic weighing scales were used to determine the fresh and dry masses. After being harvested, the roots and shoots were placed in paper bags and dried in an oven set to 75°C for at least 48 h to achieve the desired dry weight.

2.9. Biochemical analysis

2.9.1. Determination of chlorophyll and carotenoid contents

Chlorophyll and carotenoid pigments were extracted from fresh leaf tissue (0.1 g) by homogenizing in 4 mL of ice-cold 80% (v/v) acetone containing 0.1% (w/v) magnesium carbonate (to prevent pheophytin formation), followed by centrifugation at 3000 × g for 5 min at 4°C. The absorbance of the supernatant was measured at 663 nm (chlorophyll *a*), 645 nm (chlorophyll *b*), and 470 nm (carotenoids) against an 80% acetone blank using a UV-2100 spectrophotometer (Unico Co., China) with 1 cm pathlength quartz cuvettes. Pigment concentrations were calculated according to Abdel Latef et al. [34] using **Equation 2**, **Equation 3**, **Equation** 4 and **Equation 5**.

$$Chl\,a = (13.36 \times A_{663}) - (5.19 \times A_{644})\,mg/g \quad (2)$$

$$Chl\,b = (27.49 \times A_{644}) - (8.12 \times A_{663})\,mg/g \quad (3)$$

$$TC = \frac{[(1000 \times A452) - [(2.13 \times Chl\,a) - (97.64 \times Chl\,b)]}{209}\,mg/g \quad (4)$$

$$Total\ chlorophyll = [5.24 \times Abs_{663}] + Abs_{644}\ mg/g \quad (5)$$

2.9.2. Determination of total phenolic content

The total phenolic content of the leaf samples was estimated following the method described by Oloumi et al. [35] with some modifications. A 100 mg leaf sample was extracted in 5 mL of 95% ethanol and centrifuged for 5 min at 8000 rpm. The supernatant was mixed with 0.5 mL of Folin–Ciocalteu reagent prepared in a 1:1 ratio with distilled water. A total of 1.5 mL of 5% sodium carbonate solution was added to the sample, and the absorbance was measured at 725 nm spectrophotometer (UV-2100, Unico Co., China) after 1 h of incubation at room temperature, and the total phenolic content was calculated following **Equation 6** using gallic acid as standard (Fig. 1).

$$Phenolic\ content = \left[\frac{Absorbance}{0.0064} - 0.0787\right] \times dilution\ factor\ mg/g\ FW \quad (6)$$

2.9.3. Determination of anthocyanin content

Anthocyanin content was quantified using a modified protocol adapted from Oloumi et al. [35]. Fresh leaf tissue (100 mg) was homogenized in 10 mL of acidified methanol (99:1 v/v methanol:1 N HCl) and incubated in complete darkness at 25°C for 24 h to ensure complete pigment extraction while preventing photodegradation. The samples were then centrifuged at 4000 × g for 5 min at 25°C to pellet cellular debris, and the supernatant was filtered through a 0.45 µm PTFE membrane. Absorbance of the clarified extract was measured at 550 nm against a methanol:HCl blank using a UV-2100 spectrophotometer (Unico Co., China) with 1 cm pathlength quartz cuvettes. Anthocyanin concentration was calculated using the molar extinction coefficient of cyanidin-3-o-glucoside (ε = 29,600 M/cm) and expressed as micromoles per gram fresh weight (µmol/g FW) according to **Equation 7**, where the dilution factor accounted for the 10 mL extraction volume per 100 mg tissue.

$$Anthocyanin\ content = \frac{Absorbance \times Dilution\ factor}{Fresh\ weight} \times 33\ mM/g\ FW \quad (7)$$

2.9.4. Determination of catalase (CAT) activity

Catalase (CAT; EC 1.11.1.6) activity was determined by monitoring the decomposition of H_2O_2 at 240 nm [36,37], with modifications. Fresh leaf tissue (0.5 g) was homogenized in 5 mL of ice-cold 50 mM sodium phosphate buffer (pH 7.5) containing 1 mM EDTA (to prevent metal-catalyzed oxidation) using a pre-chilled mortar and pestle. The homogenate was centrifuged at 10,000 × g for 20 min at 4°C, and the supernatant was collected as the crude enzyme extract. The reaction mixture contained 1.8 mL of 50 mM sodium phosphate buffer (pH 7.5) and 1.0 mL of 15 mM H_2O_2 substrate solution (prepared by diluting 0.2 mL of 30% stock to 50 mL with buffer). The reaction was initiated by adding 0.1 mL of enzyme extract to the cuvette, and the decrease in absorbance at 240 nm was recorded every 15 s for 2 min using a UV-2100 spectrophotometer (Unico Co., China) with temperature control maintained at 25°C. One unit of CAT activity was defined as the amount of enzyme required to decompose 1 µmol of H_2O_2 per minute under the assay conditions, calculated using the extinction coefficient of 39.4 M/cm for H_2O_2. Activity was expressed as µmol H_2O_2 decomposed min/mg protein [**Equation 8**], with total protein content determined by the Bradford method [38] using BSA as standard.

$$CAT\ activity = \frac{Absorbance \times Dilution\ factor}{Fresh\ weight \times Excitation\ coefficient \times time \times protein\ content}\ \mu mol/min \quad (8)$$

2.9.5. Determination of peroxidase (POD) activity

Peroxidase (POD; EC 1.11.1.7) activity was determined by homogenizing 1.0 g fresh leaf tissue in 5 mL ice-cold 0.1 M sodium phosphate buffer (pH 6.5) containing 1% polyvinylpyrrolidone (PVP), followed by centrifugation at 10,000 × g for 20 min at 4°C; the supernatant was adjusted to 3 mL with extraction buffer and combined with 3.0 mL of 0.05 M guaiacol and 1.0 mL of 0.1 M phosphate buffer (pH 6.5) in a quartz cuvette. After adding 0.1 mL of 0.8 M H_2O_2 to initiate the reaction, the increase in absorbance at 470 nm was recorded every 15 s for 3 min at 25°C using a UV-2100 spectrophotometer (Unico Co.) [37], with activity calculated using the extinction coefficient of tetraguaiacol (26.6 mM/cm) and expressed as µmol tetraguaiacol formed min/g FW according to **Equation 9**.

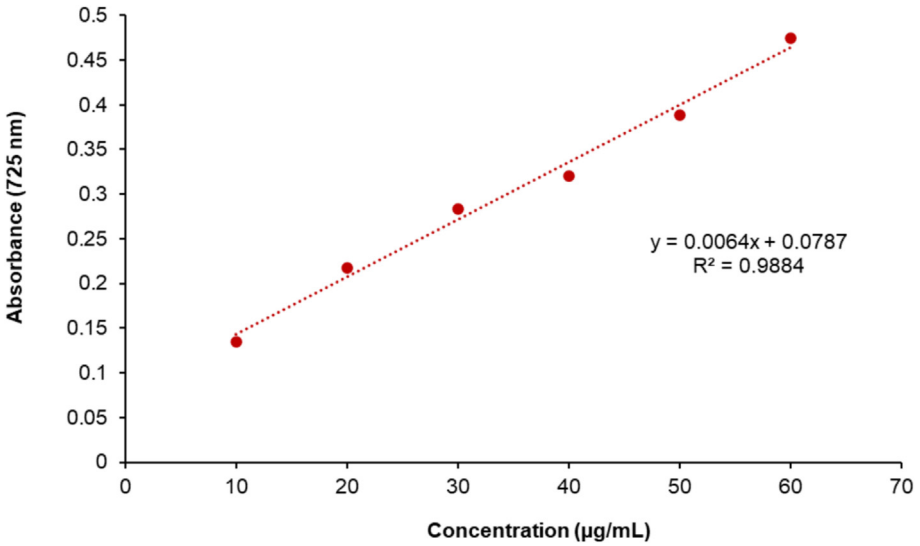

Fig. 1. Standard curve of gallic acid.

$$POD\ activity = \frac{Absorbance \times Dilution\ factor}{Fresh\ weight \times Excitation\ coefficient \times time \times protein\ content}\ \mu mol/min \quad (9)$$

2.10. Statistical analysis

To meet the requirements of a randomized design, three replicate experiments were conducted for each treatment. The statistical program Statistix 8.1 was used to evaluate the data and find any significant impacts by performing one-way analysis of variance (ANOVA) on the growth parameters and yield [39]. To investigate the statistically significant differences between the means, 95% confidence level Duncan's multiple range tests were performed [40].

3. Results

3.1. Extracellular synthesis and characterization of AgNPs by TEM

Various proportions of silver nitrate solution were amalgamated with the culture filtrate of *A. terreus* AUMC 15760 to synthesize AgNPs. The 50:50 ratio resulted in the most significant reduction of silver ions to silver nanoparticles. TEM examination revealed that the synthesized AgNPs predominantly exhibited spherical and irregular morphologies. The average dimensions of the AgNPs vary from 12.1 to 28.7 nm (Fig. 2).

3.2. In vitro effect of AgNPs on the growth of F. oxysporum AUMC 15798

The effectiveness of AgNPs against the proliferation of *F. oxysporum* AUMC 15798 was examined *in vitro* in a laboratory environment. These findings indicate that AgNPs hindered the growth of *F. oxysporum* AUMC 15798 to varying extents and considerably diminished the formation of the pathogen lining. The application of 200 ppm AgNPs resulted in the highest percentage of radial growth inhibition at 69.33%, followed by 150 ppm AgNPs at 54.44%. Moreover, 100 ppm AgNPs resulted in a moderate reduction in radial growth (40.77%), whereas 50 ppm AgNPs resulted in the lowest percentage of growth inhibition (24.88%). The application of identical concentrations (50, 100, 150, and 200 ppm) of 50% Dovex led to growth inhibition rates of 44.88%, 54.11%, 57.44%, and 83.0%, respectively (Table 1).

3.3. Greenhouse experiment

A greenhouse experiment was performed to verify the efficacy of AgNPs against *F. oxysporum* AUMC 15798. These findings suggest that AgNPs may reduce the severity of basal rot disease. Compared with the infected control (T8), the percentage of illness severity was considerably reduced to 20% after Dovex (50%) treatment (T6). Treatment with 50 ppm AgNPs (applied to soil and as a spray) diminished disease severity to 57.77% and 35.55%, respectively, whereas 100 ppm AgNPs (applied to soil and as a spray) decreased disease severity to 31.1% and 22.2%, respectively (Fig. 3).

3.4. Determination of the agronomic parameters

3.4.1. Shoot and root length

The negative control (T7) had the most significant effects on shoot and root length, with values of 62.62 cm and 20.62 cm, respectively. The Dovex (50%) (T6) treatment resulted in a shoot length of 49.97 cm and a root length of 15.48 cm, whereas the application of AgNPs at a concentration of 100 ppm (T1) surpassed that of T7, resulting in a shoot length of 57.62 cm and a root length of 17.62 cm. Conversely, treatment T8 (infected control) resulted in the least favorable outcomes for shoot length at 28.00 cm and root length at 0.76 cm (Fig. 4A,B).

3.4.2. Diameter of the onion neck

The plants subjected to 100 ppm soil treatment with AgNPs (T3) presented the greatest onion neck diameter, measuring 1.61 cm. This measurement exceeded those of the other treatments, although not in a statistically significant manner (Fig. 4C). More-

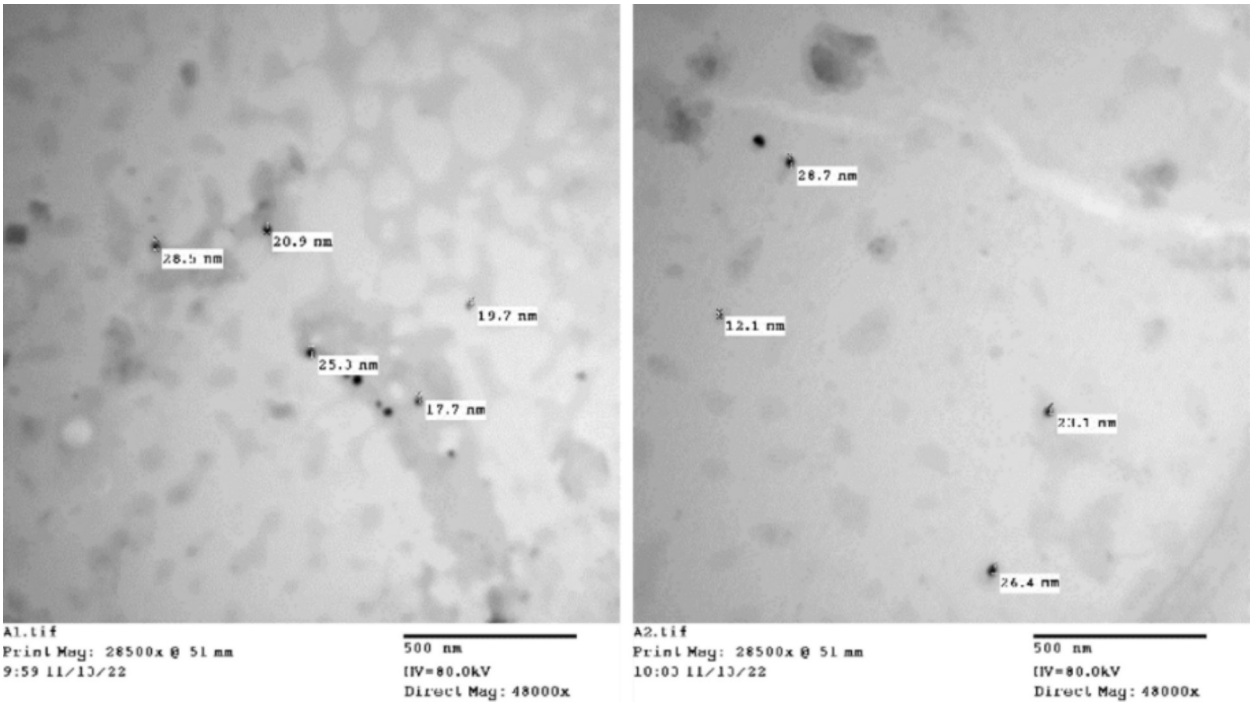

Fig. 2. TEM images of the AgNPs synthesized extracellularly by *A. terreus* AUMC 15760.

Table 1
In vitro effects of AgNPs on the radial growth of *F. oxysporum* AUMC 15798. Each value represents the mean of three replicates ± SD; values with different letters are significantly different ($p \leq 0.05$).

Treatments	Concentrations (ppm)	Colony diameter (cm)	% Inhibition
AgNPs	50	6.76 ± 0.25[b]	24.88
	100	5.33 ± 0.29[c]	40.77
	150	4.1 ± 0.10[d]	54.44
	200	2.76 ± 0.25[e]	69.33
Dovex (50%)	50	4.97 ± 0.84[c]	44.88
	100	4.13 ± 0.06[d]	54.11
	150	3.83 ± 0.29[d]	57.44
	200	1.53 ± 0.06[f]	83.00
Control		9.0 ± 0.00[a]	0.0
LSD (5%)	0.38		

[(a-f)] Each value represents the mean of three replicates ± SD; values with different letters are significantly different.

over, compared with the other treatments, the negative control (T7), application of 100 ppm AgNPs (T1), and soil treatment with Dovex (50%) resulted in no significant variation in leaf count (7.33, 6.33, and 6.0, respectively) except for T8 (4.33) (Fig. 4D).

3.4.3. Length and diameter of the bulb

The plants in the negative control group (T7) had a maximum bulb length of 4.57 cm and a diameter of 4.66 cm. A 100 ppm AgNP (T1) spray yielded bulbs measuring 4.07 cm in length and 4.16 cm in diameter. The T1 runner with a soil application of 50 ppm AgNPs (T4) presented a bulb length of 3.86 cm and a bulb width of 4.10 cm. The bulb length and diameter of the infected control (T8) were 2.65 cm and 2.54 cm, respectively, representing the lowest values for these parameters (Fig. 4E,F).

3.4.4. Plant fresh and dry weights

The negative control (T7) yielded the highest plant fresh weight, with results not significantly different from those of treatments T1 (100 ppm AgNP spray), T4 (50 ppm AgNP soil application), and T5 (Dovex 50% spray) (Fig. 4G). Compared with the infected control (T8), treatments T1, T4, and T5 presented increases in coefficients of 273.33%, 353.33%, and 333.33%, respectively. Similarly, the T7 treatment resulted in the greatest plant dry weight, which was not significantly different from those of the T1, T4, and T5 treatments. The T1, T4, and T5 coefficients increased by 280.00%, 300.33%, and 283.33%, respectively, compared with those of the infected control (Fig. 3 and Fig. 4).

3.5. Biochemical analysis

3.5.1. Determination of photosynthetic pigments

In terms of the chlorophyll *a*, chlorophyll *b*, and carotenoid concentrations, the negative control (T7) presented the highest photosynthetic content, with values of 3.21, 1.02, and 2.21 mg/g, respectively. Onion plants treated with a 100 ppm AgNP spray (T1) presented increased chlorophyll *a*, chlorophyll *b*, and carotenoid contents. The concentrations of these components were 2.99, 0.76, and 1.96 mg/g, respectively, for all three samples. Following the soil application of 50 ppm AgNPs (T4), the concentrations of chlorophyll *a*, chlorophyll *b*, and carotenoids were 2.88, 0.88, and 1.76 mg/g, respectively (Fig. 5).

3.5.2. Determination of phenolic contents

This study investigated the phenolic content of onion plants infected with *F. oxysporum* AUMC 15798 and their responses to green-synthesized silver nanoparticles (AgNPs). Compared with that in noninfected plants (T7), the phenolic content in T8 (plants under infection stress) significantly increased, measuring 0.42 mg/g. The application of AgNPs resulted in a reduction in phenolic content. Plants subjected to 50 ppm AgNPs via soil application and 100 ppm AgNPs through spraying (T4 and T6) presented the most significant reduction in phenolic content, with values of 0.31 and 0.34 mg/g, respectively (Fig. 6A).

3.5.3. Determination of anthocyanin content

The total anthocyanin content of plants subjected to infection stress (T8) increased (0.63 mg/g); however, exposure to AgNPs resulted in a considerable reduction in anthocyanin content. Plants subjected to 50 ppm AgNPs via soil application and 100 ppm AgNPs through spraying of biosynthesized AgNPs (T4 and T6) presented the most significant reduction in anthocyanin content, with values of 0.46 and 0.48 mg/g, respectively (Fig. 6B).

3.5.4. Determination of peroxidase (POD) activity

The results indicated that, compared with the negative control plants, the infected control onion plants presented elevated levels of POD and CAT. The POD activity in the infected plants increased to 0.77 µmol/min. The plants subjected to 50 ppm AgNPs via soil

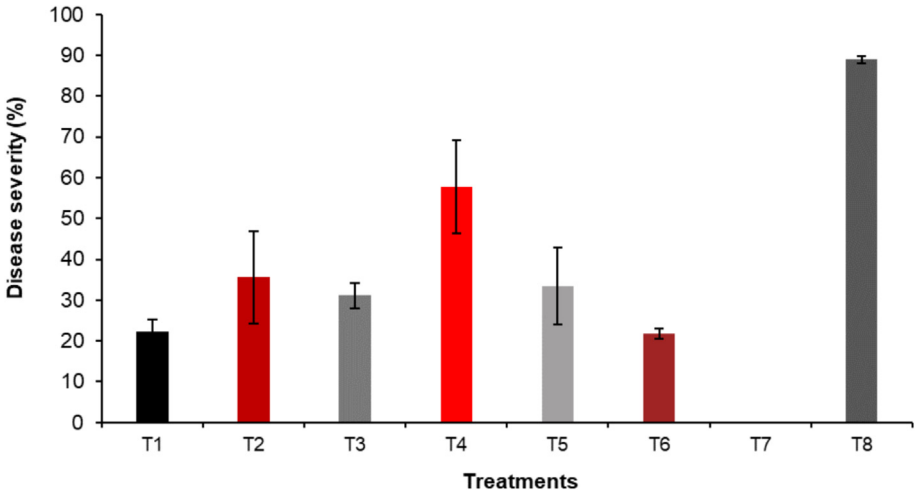

Fig. 3. Percentage severity of basal rot disease on onion plants treated with AgNPs and Dovex (50%) under greenhouse conditions (mean values ± SDs on bar graphs with different letters are significantly different ($p \leq 0.05$; n = 3; T1 = 100 ppm AgNPs (Spray); T2 = 50 ppm AgNPs (Spray); T3 = 100 ppm AgNPs (Soil application); T4 = 50 ppm AgNPs (Soil application); T5 = Spray of Dovex (50%); T6 = Soil application of Dovex (50%); T7 = Negative control; T8 = Infected control).

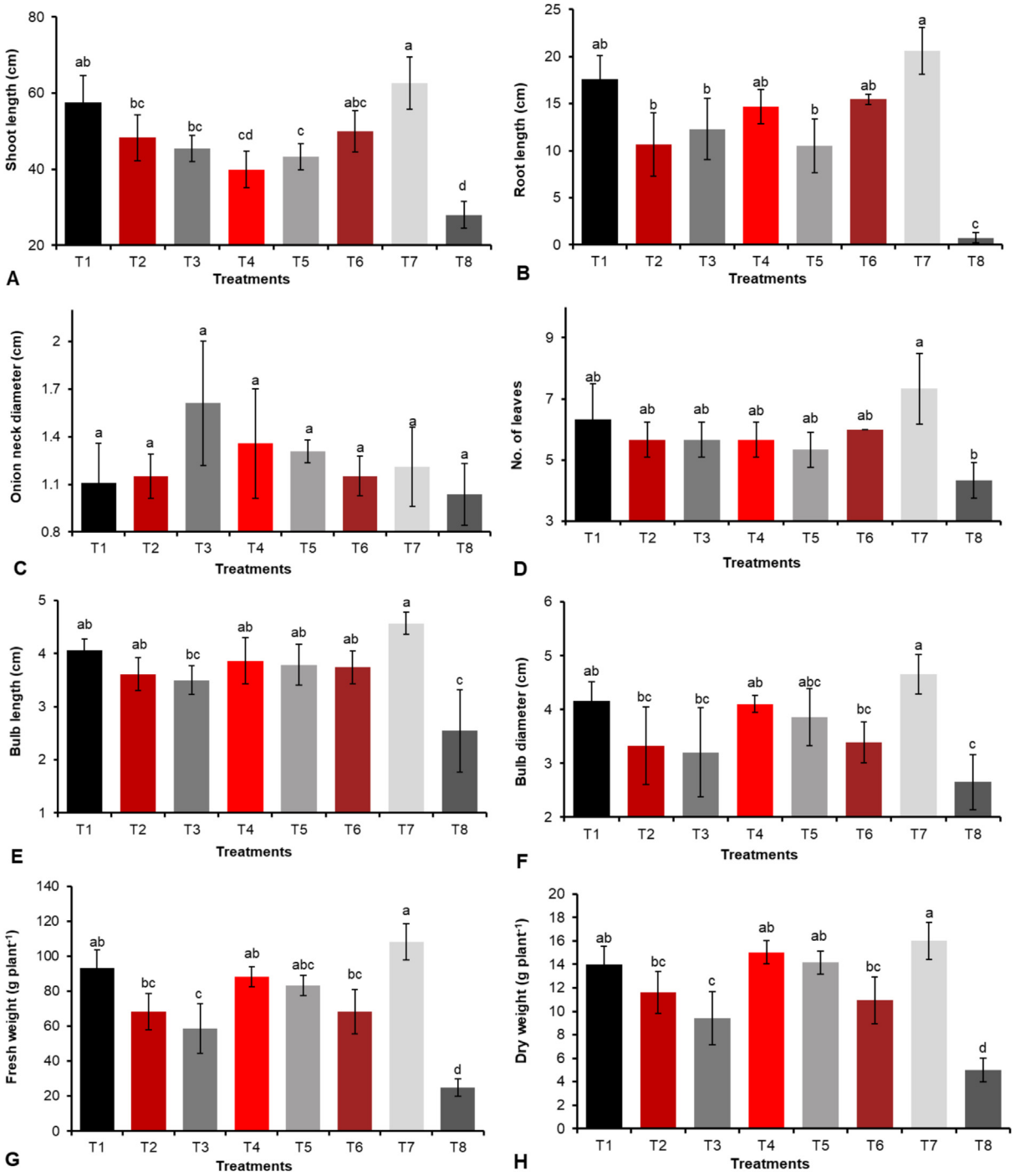

Fig. 4. Effect of AgNPs and 50% Dovex on the growth parameters of onion plants infected with *F. oxysporum* AUMC 15798 under greenhouse conditions: (A), shoot length; (B), root length; (C), onion neck; (D), diameter of leaves; (E), bulb length; (F), bulb diameter; (G), plant fresh weight; (H), plant dry weight (mean values ± SDs on bar graphs with different letters are significantly different ($p \leq 0.05$; n = 3; T1 = 100 ppm AgNPs (Spray); T2 = 50 ppm AgNPs (Spray); T3 = 100 ppm AgNPs (Soil application); T4 = 50 ppm AgNPs (Soil application); T5 = Spray of Dovex (50%); T6 = Soil application of Dovex (50%); T7 = Negative control; T8 = Infected control).

application (T4) and 100 ppm AgNPs through spraying (T1) presented the most significant reduction, with values of 0.49 and 0.44 µmol/min/g, respectively (Fig. 7A).

3.5.5. Determination of catalase (CAT) activity

These results demonstrated that the application of AgNPs reduced the synthesis of native enzymes. The most significant decrease in CAT content occurred in onion plants treated with 100 ppm AgNPs via spray and 50 ppm AgNPs through soil application (T1 and T4), with values of 0.19 and 0.22 µmoles min/g, respectively. The application of Dovex soil at 50% (T6) resulted in a reduction in the CAT content to 0.22 µmoles min/g, in contrast to the CAT activity of the positive control, which was 0.35 µmol/min/g (Fig. 7B).

4. Discussion

There is an urgent need to search for and create alternative eco-friendly, safe, and effective plant disease control methods, such as onion basal rot disease, that may be integrated into root-rot dis-

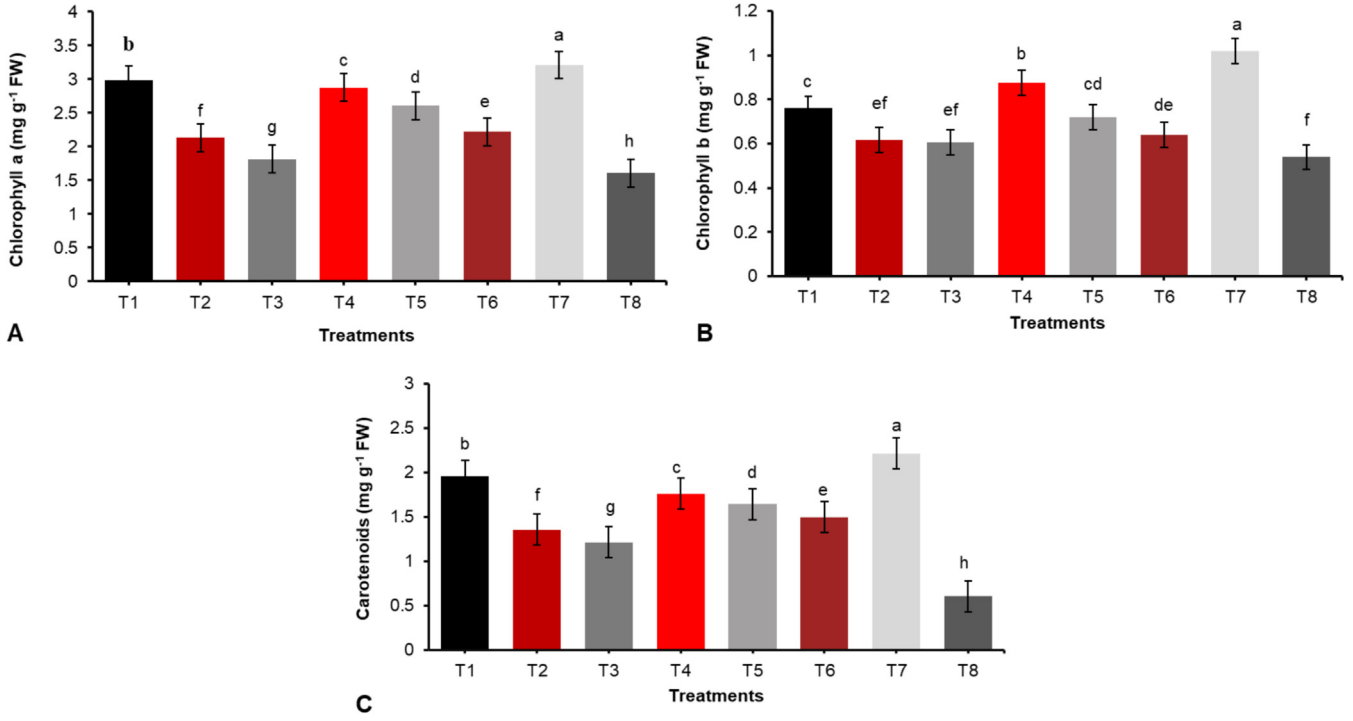

Fig. 5. Effect of AgNPs and Dovex 50% on photosynthetic pigments in onion plants infected with *F. oxysporum* AUMC 15798 under greenhouse conditions: (A), chlorophyll *a*; (B), chlorophyll *b*; (C), carotenoid content (mean values ± SDs on bar graphs with different letters are significantly different ($p \leq 0.05$; n = 3; T1 = 100 ppm AgNPs (Spray); T2 = 50 ppm AgNPs (Spray); T3 = 100 ppm AgNPs (Soil application); T4 = 50 ppm AgNPs (Soil application); T5 = Spray of Dovex (50%); T6 = Soil application of Dovex (50%); T7 = Negative control; T8 = Infected control).

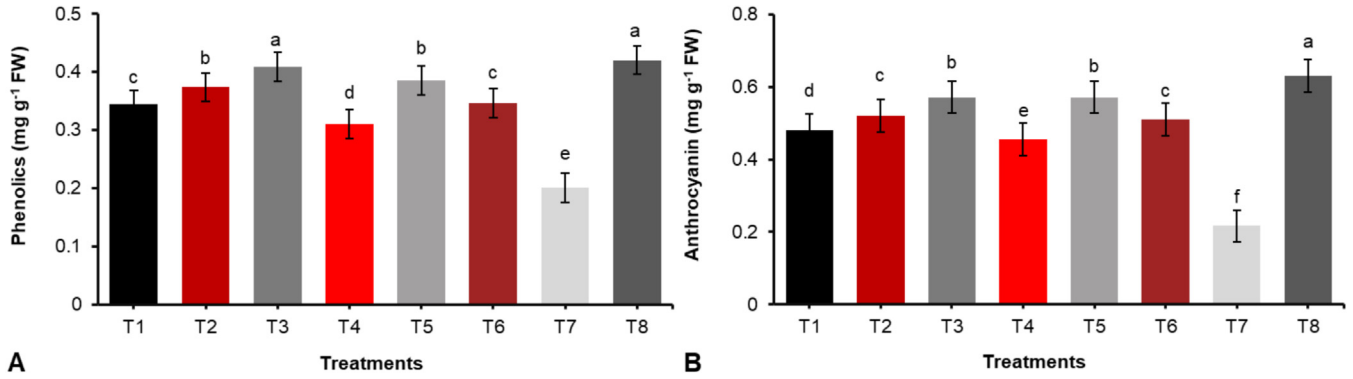

Fig. 6. Effect of AgNPs and Dovex 50% on nonenzymatic antioxidant activities in onion plants infected with *F. oxysporum* AUMC 15798 under greenhouse conditions: (A), phenolic contents; (B), anthocyanin content (mean values ± SDs on bar graphs with different letters are significantly different ($p \leq 0.05$; n = 3; T1 = 100 ppm AgNPs (Spray); T2 = 50 ppm AgNPs (Spray); T3 = 100 ppm AgNPs (Soil application); T4 = 50 ppm AgNPs (Soil application); T5 = Spray of Dovex (50%); T6 = Soil application of Dovex (50%); T7 = Negative control; T8 = Infected control).

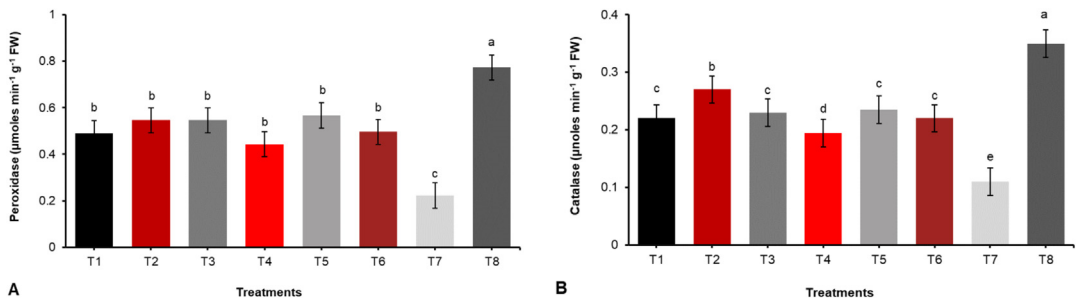

Fig. 7. Effect of AgNPs and Dovex 50% on enzymatic antioxidant activities in onion plants infected with *F. oxysporum* AUMC 15798 under greenhouse conditions: (A), POD; (B), CAT (mean values ± SDs on bar graphs with different letters are significantly different ($p \leq 0.05$; n = 3; T1 = 100 ppm AgNPs (Spray); T2 = 50 ppm AgNPs (Spray); T3 = 100 ppm AgNPs (Soil application); T4 = 50 ppm AgNPs (Soil application); T5 = Spray of Dovex (50%); T6 = Soil application of Dovex (50%); T7 = Negative control; T8 = Infected control).

ease management programs. The successful isolation of *F. oxysporum* from infected onion plants is a critical step in discovering the cause of the disease [41]. The *F. oxysporum* strain AUMC 15798 was isolated and determined to be the most harmful, with a disease severity rate of 88.88% [21]. As a result, it was chosen for this research. It is estimated that *F. oxysporum* has approximately 120 different strains or forms, each of which is unique to the host plant it infects. Gymnosperms, angiosperms, monocots, and dicots are among its diverse spectrum of hosts [42,43,44,45,46,47,48,49].

In this study, laboratory experiments evaluating the effects of AgNPs on *F. oxysporum* revealed a clear antifungal effect. The dose-dependent inhibition of fungal growth with increasing concentrations of AgNPs (200 ppm > 150 ppm > 100 ppm > 50 ppm) was an important result. At 200 ppm, AgNPs had the highest percentage of inhibition (69.33%), indicating their promise as antifungal agents against this disease. Nanomaterials have been used more recently, and their potential as substitutes for treating plant diseases is being explored.

Extensive research has demonstrated the potent antifungal properties of metallic nanoparticles, particularly silver nanoparticles (AgNPs), against diverse plant pathogenic fungi. Multiple studies have confirmed that AgNPs exhibit broad-spectrum antimicrobial activity, effectively suppressing key phytopathogens such as *F. oxysporum*, *B. cinerea*, and *Alternaria alternata* [50,51,52]. Notably, time-dependent efficacy studies revealed that AgNP application 3 h post-inoculation significantly reduced disease severity by inhibiting fungal growth in *Magnaporthe grisea* and *Bipolaris sorokiniana*, though this protective effect diminished when treatment was delayed to 24 h [53].

AgNPs have shown remarkable effectiveness against both foliar and soil-borne pathogens, including *Pythium spinosum* and *Fusarium* spp., through dose-dependent inhibition of conidial germination and mycelial growth [54,55]. Citrus pathogen studies further validated their activity against *Alternaria citri* and *Penicillium digitatum*, highlighting their potential as versatile antifungal agents in agriculture [56]. These findings underscore AgNPs' dual role as both direct fungicides and plant defense enhancers against economically significant crop diseases.

Dovex 50% fungicide and silver nanoparticles at 50, 100, and 150 ppm were added to PDA media prior to the *in vitro* experiment. Comparative studies demonstrated that silver nanoparticles (AgNPs) outperformed traditional fungicides in inhibiting fungal growth. Notably, biologically synthesized AgNPs (800 μL/L) derived from *Trichoderma harzianum* effectively suppressed both mycelial growth and sporulation of *F. oxysporum* f. sp. *Lycopersici in vitro*, confirming their superior antifungal properties [57]. Field-relevant applications showed similar efficacy, with 50 ppm AgNPs reducing purple blotch disease severity (caused by *Alternaria porri*) from 85.5% to 23.38% – a 72.6% reduction in infection rates [33].

The greenhouse experiments provided more evidence that AgNPs have the ability to reduce onion basal rot disease. The disease severity was reduced to 57.77% and 35.55%, respectively, after treatment with 50 ppm AgNPs (soil application and spray) and to 31.11% and 33.33%, respectively, after treatment with 100 ppm AgNPs (soil application and spray). The observed antifungal effects of silver nanoparticles (AgNPs) may be attributed to their ability to disrupt fungal cell membranes and inhibit fungal growth [58]. Although the exact antimicrobial mechanism of AgNPs remains under debate, several theories have been proposed to explain their mode of action [59]. One widely accepted hypothesis suggests that AgNPs can attach to the surface of fungal cells and subsequently penetrate the membrane, increasing its permeability and ultimately leading to cell death [60]. Another proposed mechanism involves the generation of reactive oxygen species (ROS) or free radicals by AgNPs, which can damage cellular components and further compromise membrane integrity, resulting in cell lysis [61,62].

It has also been suggested that silver nanoparticles (AgNPs) release silver ions (Ag^+), which contribute significantly to their antimicrobial activity [63]. These ions can bind to thiol (—SH) groups in essential enzymes, leading to enzyme inactivation and disruption of vital cellular processes [64]. Silver, being a soft acid, naturally interacts with soft bases such as sulfur and phosphorus, which are abundant in cellular structures [65]. This interaction allows Ag^+ to target cellular components like proteins and membranes, ultimately causing cell damage and death. Furthermore, since DNA contains sulfur and phosphorus, AgNPs may interfere with DNA replication by binding to these elements, potentially resulting in mutations or cell death [66].

Silver nanoparticles produce antimicrobial silver ions that interfere with the function of cell wall proteins. Additionally, these nanoparticles may adhere to proteins in the outermost membrane, forming complexes with oxygen, phosphorus, nitrogen, or sulfur-containing groups. This interaction, particularly involving disulfide bonds, causes the inactivation of enzymes and proteins situated in the membrane, eventually clogging their active sites [67,68].

The chlorophyll *a*, chlorophyll *b*, and carotenoid contents were all reduced in this study because of basal rot disease. The application of 50 ppm AgNPs (soil application) and 100 ppm AgNPs (spray) to onion plants resulted in increased chlorophyll *a*, chlorophyll *b*, and carotenoid contents. These findings suggest that the use of AgNPs enhances photosynthetic pigments in onion plants while lessening the negative effects of fungal infection. Research demonstrating that foliar application of AgNPs increased photosynthetic pigments (carotenoid, chlorophyll, a and b) in fenugreek plants (*Trigonella foenum-graecum*) corroborated our findings [69]. Additionally, we analyzed anthocyanin and phenolic contents in plants affected by basal rot disease in response to green-synthesized AgNPs. Disease stress increased the phenolic content to 0.42 mg/g, while AgNP treatment reduced it, with the 50 ppm treatment showing the greatest decrease (0.31 mg/g). A similar trend was observed for anthocyanin content, which showed a strong linear relationship with total phenolic levels. Furthermore, biologically produced AgNPs significantly affect seed germination, increase the synthesis of carbohydrates and protein, and decrease the total phenol content in *Bacopa monnieri* [70].

Phenolic compounds –including flavonoids, anthocyanins, and tannins- exhibit antioxidant properties by scavenging reactive oxygen species (ROS), thereby preventing or mitigating oxidative stress in plant cells [71]. In this study, onion plants infected with *Fusarium* showed elevated levels of catalase (CAT) and peroxidase (POD) compared to the healthy control, indicating a heightened antioxidant response to fungal stress. However, the application of biosynthesized silver nanoparticles (AgNPs) appeared to reduce the levels of these endogenous enzymes. Specifically, CAT and POD activities were noticeably lower in plants treated with 50 ppm AgNPs (soil application) and 100 ppm AgNPs (foliar spray). This suggests that AgNPs may alleviate oxidative stress, reducing the need for elevated antioxidant enzyme production. In contrast, Abd-Ellatif et al. [72] reported increased CAT and POD activities in plants treated with *Thymus vulgaris* essential oil-loaded chitosan nanoparticles (ThE-CsNPs) against *Fusarium solani*. These differences highlight the potential of AgNPs as a biocontrol agent that supports the plant's defense by effectively limiting ROS accumulation during biotic stress.

Overall, our findings revealed how effective AgNPs may be in preventing onion basal rot disease and enhancing the physiology and growth of plants. AgNPs have the potential to be effective tools in agriculture for managing diseases and improving crop production, as evidenced by their dose-dependent antifungal activity and favorable impacts on morphological parameters and photo-

synthetic pigments. On the other hand, given the complexity of the interactions between AgNPs and nonenzymatic antioxidants, more research is needed. Furthermore, the ability of AgNPs to control antioxidant enzyme activity demonstrated how they help infected plants develop disease resistance by lowering oxidative stress.

5. Conclusions

AgNPs have been demonstrated in greenhouse trials to significantly reduce the severity of onion basal rot disease when used as a soil treatment. AgNPs increased the overall biomass, bulb size, and length of shoots and roots of onion plants. Similarly, the photosynthetic pigment content was increased by the AgNP treatment. AgNPs influence anthocyanins and phenolic compounds, suggesting their potential role in lowering the oxidative stress caused by fungal infection. On the other hand, research has shown that AgNPs reduce POD and CAT activity, suggesting a modification in the plant's defense mechanisms. Overall, the results of this study revealed how AgNPs have various effects on onion plants and how integrated management strategies could be employed to prevent onion basal rot disease. Further study is needed to fully understand the mechanisms underlying these advantages and to make most AgNPs suitable for agricultural practices.

CRediT authorship contribution statement

Mohamed G.A. Hegazy: Writing – original draft, Data curation, Investigation, Methodology, Conceptualization. **Mahmoud Gad:** Methodology, Conceptualization, Investigation, Writing – original draft, Data curation. **Sobhi F. Lamlom:** Investigation, Writing – original draft, Data curation, Methodology. **Islam I. Teiba:** Writing – original draft, Methodology, Data curation, Investigation. **Osama A.M. Al-Bedak:** Writing – original draft, Data curation, Investigation, Methodology, Conceptualization, Formal analysis, Software. **Muhammad Moaaz Ali:** Validation, Data curation, Writing – original draft, Formal analysis. **Eman Alhomaidi:** Formal analysis, Data curation, Funding acquisition. **Mona Saleh Al Tami:** Formal analysis, Data curation, Funding acquisition. **Ahmed F. Yousef:** Data curation, Formal analysis, Writing – original draft, Investigation, Methodology, Conceptualization. **Waleed M. Ali:** Methodology, Investigation, Conceptualization, Writing – original draft, Data curation, Formal analysis.

Financial support

This work was funded by Princess Nourah bint Abdulrahman University Researchers Supporting Project number (PNURSP2025R317), Princess Nourah bint Abdulrahman University, Riyadh, Saudi Arabia.

Declaration of competing interest

The authors declare that they have no known competing financial interests or personal relationships that could have appeared to influence the work reported in this paper.

Supplementary material

https://doi.org/10.1016/j.ejbt.2025.05.003.

Data availability

Data will be made available on request.

References

[1] Chakraborty AJ, Uddin TM, Zidan BRM, et al. *Allium cepa*: A treasure of bioactive phytochemicals with prospective health benefits. Evid Based Complement Alternat Med 2022;2022(1):4586318. https://doi.org/10.1155/2022/4586318. PMid: 35087593.
[2] Sami R, Elhakem A, Alharbi M, et al. Nutritional values of onion bulbs with some essential structural parameters for packaging process. Appl Sci 2021;11(5):2317. https://doi.org/10.3390/app11052317.
[3] Sharma S, Mandal S, Cramer CS. Recent advances in understanding and controlling *Fusarium* diseases of alliums. Horticulturae 2024;10(5):527. https://doi.org/10.3390/horticulturae10050527.
[4] Edel-Hermann V, Lecomte C. Current status of *Fusarium oxysporum formae speciales* and races. Phytopathology 2019;109(4):512–30. https://doi.org/10.1094/PHYTO-08-18-0320-RVW. PMid: 30461350.
[5] Rongai D, Pulcini P, Pesce B, et al. Antifungal activity of some botanical extracts on *Fusarium oxysporum*. Open Life Sci 2015;10(1):409–16. https://doi.org/10.1515/biol-2015-0040.
[6] Nosrati H, Aramideh Khouy R, Nosrati A, et al. Nanocomposite scaffolds for accelerating chronic wound healing by enhancing angiogenesis. J Nanobiotechnol 2021;19:1. https://doi.org/10.1186/s12951-020-00755-7. PMid: 33397416.
[7] Thiruvengadam M, Rajakumar G, Chung I-M. Nanotechnology: Current uses and future applications in the food industry. 3 Biotech 2018;8:1–13. https://doi.org/10.1007/s13205-018-1104-7. PMid: 29354385.
[8] Saxena J, Sharma MM, Gupta S, et al. Emerging role of fungi in nanoparticle synthesis and their applications. World J Pharm Sci 2014;3(9):1586–613.
[9] Elgorban AM, El-Samawaty A-E-R-M, Yassin MA, et al. Antifungal silver nanoparticles: Synthesis, characterization and biological evaluation. Biotechnol Biotechnol Equip 2016;30(1):56–62. https://doi.org/10.1080/13102818.2015.1106339.
[10] Elblbesy M-A-A, Madbouly AK, Hamdan T-A-A. Bio-synthesis of magnetite nanoparticles by bacteria. Am J Nano Res Appl 2014;2(5):98–103.
[11] Yassin MA, Elgorban AM, El-Samawaty AE-RM, et al. Biosynthesis of silver nanoparticles using *Penicillium verrucosum* and analysis of their antifungal activity. Saudi J Biol Sci 2021;28(4):2123–7. https://doi.org/10.1016/j.sjbs.2021.01.063. PMid: 33911928.
[12] Siddiqi KS, Husen A. Fabrication of metal nanoparticles from fungi and metal salts: Scope and application. Nanoscale Res Lett 2016;11:98. https://doi.org/10.1186/s11671-016-1311-2. PMid: 26909778.
[13] Malik MA, Wani AH, Bhat MY, et al. Fungal-mediated synthesis of silver nanoparticles: A novel strategy for plant disease management. Front Microbiol 2024;15:1399331. https://doi.org/10.3389/fmicb.2024.1399331. PMid: 39006753.
[14] Anjum S, Vyas A, Sofi T. Fungi-mediated synthesis of nanoparticles: Characterization process and agricultural applications. J Sci Food Agric 2023;103(10):4727–41. https://doi.org/10.1002/jsfa.12496. PMid: 36781932.
[15] Tariq M, Mohammad KN, Ahmed B, et al. Biological synthesis of silver nanoparticles and prospects in plant disease management. Molecules 2022;27(15):4754. https://doi.org/10.3390/molecules27154754. PMid: 35897928.
[16] Buggana A, Bandari K, Golla N, et al. Leaf-mediated green synthesis of silver nanoparticles from *Azadirachta indica* and *Ficus religiosa*: Characterization and bioactive properties. Egypt J Agric Res 2024;102(3):392–406. https://doi.org/10.21608/ejar.2024.285666.1541.
[17] Nasr A, Yousef AF, Hegazy MGA, et al. Biosynthesized silver nanoparticles mitigate charcoal rot and root-knot nematode disease complex in faba bean. Physiol Mol Plant Pathol 2025;136:102610. https://doi.org/10.1016/j.pmpp.2025.102610.
[18] Francis S, Joseph S, Koshy EP, et al. Microwave assisted green synthesis of silver nanoparticles using leaf extract of *Elephantopus scaber* and its environmental and biological applications. Artif Cells Nanomed Biotechnol 2018;46(4):795–804. https://doi.org/10.1080/21691401.2017.1345921. PMid: 28681662.
[19] Siddiqi KS, Husen A, Rao RA. A review on biosynthesis of silver nanoparticles and their biocidal properties. J Nanobiotechnol 2018;16:14. https://doi.org/10.1186/s12951-018-0334-5. PMid: 29452593.
[20] Zhao X, Zhou L, Riaz Rajoka MS, et al. Fungal silver nanoparticles: Synthesis, application and challenges. Crit Rev Biotechnol 2018;38(6):817–35. https://doi.org/10.1080/07388551.2017.1414141. PMid: 29254388.
[21] Hegazy MG, Ahmed A-RM, Yousef AF, et al. Effectiveness of some plant extracts in biocontrol of induced onion basal rot disease in greenhouse conditions. AMB Express 2024;14(1):72. https://doi.org/10.1186/s13568-024-01721-4. PMid: 38874641.
[22] Ramadan AM, Shehata RM, El-Sheikh HH, et al. Exploitation of sugarcane bagasse and environmentally sustainable production, purification, characterization, and application of lovastatin by *Aspergillus terreus* AUMC 15760 under solid-state conditions. Molecules 2023;28(10):4048. https://doi.org/10.3390/molecules28104048. PMid: 37241788.
[23] Smith D, Onions AH. In: The preservation and maintenance of living fungi. Wallingford, UK: CAB International; 1994. https://doi.org/10.1079/9780851989020.0000.
[24] Al-Bedak OA, Sayed RM, Hassan SH. A new low-cost method for long-term preservation of filamentous fungi. Biocatal Agric Biotechnol 2019;22:101417. https://doi.org/10.1016/j.bcab.2019.101417.

[25] Hamad M. Biosynthesis of silver nanoparticles by fungi and their antibacterial activity. Int J Environ Sci Technol 2019;16:1015–24. https://doi.org/10.1007/s13762-018-1814-8.
[26] Banala RR, Nagati VB, Karnati PR. Green synthesis and characterization of *Carica papaya* leaf extract coated silver nanoparticles through X-ray diffraction, electron microscopy and evaluation of bactericidal properties. Saudi J Biol Sci 2015;22(5):637–44. https://doi.org/10.1016/j.sjbs.2015.01.007. PMid: 26288570.
[27] Macías Sánchez KL, González Martínez HDR, Carrera Cerritos R, et al. *In vitro* evaluation of the antifungal effect of AgNPs on *Fusarium oxysporum* f. sp. *lycopersici*. Nanomaterials 2023;13(7):1274. https://doi.org/10.3390/nano13071274. PMid: 37049367.
[28] Abd-Elaziz MA, Aly M-M-E-S, Mohamed A-E-A. Biological control of some garlic diseases using antagonistic fungi and bacteria. J Phytopathol Dis Manag 2021;8(1):46–63.
[29] Hussein RR, Aly M-M-E-S, Mohamed A-E-A. Effect of some biofertilizers and biofungicides applications on control onion root-rot disease. J Phytopathol Dis Manag 2021;8(1):15–28.
[30] Shieh G, Jan SL. The effectiveness of randomized complete block design. Stat Neerl 2004;58(1):111–24. https://doi.org/10.1046/j.0039-0402.2003.00109.x.
[31] AlAita A, Talebi H. Exact neutrosophic analysis of missing value in augmented randomized complete block design. Complex Intell Syst 2024;10(1):509–23. https://doi.org/10.1007/s40747-023-01182-5.
[32] El-Naggar A, El-Sheikh Aly M, El-Emary F, et al. Disease management of rose powdery mildew using some fungicides and biofungicides. Arch Agric Sci J 2023;6(2):44–57. https://doi.org/10.21608/aasj.2023.304185.
[33] Ahmed HA, Hassan MA, Hussein MA, et al. Efficiency of bio-agents and green-synthesized silver nanoparticles in controlling purple blotch disease caused by *Alternaria porri* in onion plants. Not Scientia Biol 2024;16(2):11854. https://doi.org/10.55779/nsb16211854.
[34] Abdel Latef AAH, Abu Alhmad MF, Kordrostami M, et al. Inoculation with *Azospirillum lipoferum* or *Azotobacter chroococcum* reinforces maize growth by improving physiological activities under saline conditions. J Plant Growth Regul 2020;39(3):1293–306. https://doi.org/10.1007/s00344-020-10065-9.
[35] Oloumi H, Soltaninejad R, Baghizadeh A. The comparative effects of nano and bulk size particles of CuO and ZnO on glycyrrhizin and phenolic compounds contents in *Glycyrrhiza glabra* L. seedlings. Indian J Plant Physiol 2015;20:157–61. https://doi.org/10.1007/s40502-015-0143-x.
[36] Kadhum MA, Hadwan MH. A precise and simple method for measuring catalase activity in biological samples. Chem Pap 2021;75:1669–78. https://doi.org/10.1007/s11696-020-01401-0.
[37] Alici EH, Arabaci G. Determination of SOD, POD, PPO and cat enzyme activities in *Rumex obtusifolius* L. Annu Res Rev Biol 2016;11(3):1–7. https://doi.org/10.9734/ARRB/2016/29809.
[38] Bradford MM. A rapid and sensitive method for the quantitation of microgram quantities of protein utilizing the principle of protein-dye binding. Anal Biochem 1976;72(1):248–54. https://doi.org/10.1016/0003-2697(76)90527-3. PMid: 942051.
[39] Brantmeier C. Statistical procedures for research on L2 reading comprehension: An examination of ANOVA and Regression Models. Read Foreign Lang 2004;16(2):51–69.
[40] Tallarida RJ, Murray RB, Tallarida RJ, et al. In: Duncan multiple range test. New York, NY: Springer; 1987. p. 125–7. https://doi.org/10.1007/978-1-4612-4974-0_38.
[41] El-Debaiky SA, El-Sayed AF. Morphological and molecular identification of endophytic fungi from roots of tomato and evaluation of their antioxidant and cytotoxic activities. Egypt J Bot 2023;63(3):981–1003. https://doi.org/10.21608/ejbo.2023.201958.2291.
[42] Zhu Y, Lujan P, Wedegaertner T, et al. First report of *Fusarium oxysporum* f. sp. *vasinfectum* race 4 causing Fusarium wilt of cotton in New Mexico, USA. Plant Dis 2020;104(2):588. https://doi.org/10.1094/PDIS-06-19-1170-PDN.
[43] Ploetz RC. *Fusarium wilt* of banana. Phytopathology 2015;105(12):1512–21. https://doi.org/10.1094/PHYTO-04-15-0101-RVW. PMid: 26057187.
[44] Chen Y, Lin Y, Chung W. Fusarium wilt of basil caused by *Fusarium oxysporum* f. sp. *basilici* in Taiwan. Plant Med 2017;59(1–2):1–5.
[45] Salim HA, Salman IS, Jasim BN. IPM approach for the management of wilt disease caused by *Fusarium oxysporum* f. sp. *lycopersici* on tomato (*Lycopersicon esculentum*). J Exp Biol Agric Sci 2016;4:742–7. https://doi.org/10.18006/2016.4(VIS).742.747.
[46] Basco M, Bisen K, Keswani C, et al. Biological management of *Fusarium wilt* of tomato using biofortified vermicompost. Mycosphere 2017;8(3):467–83. https://doi.org/10.5943/mycosphere/8/3/8.
[47] Guerrero M, Martínez M, León M, et al. First report of *Fusarium wilt* of lettuce caused by *Fusarium oxysporum* f. sp. *lactucae* race 1 in Spain. Plant Dis 2020;104(6):1858. https://doi.org/10.1094/PDIS-10-19-2143-PDN.
[48] Rolim J, Savian L, Walker C, et al. First report of *Fusarium wilt* caused by *Fusarium oxysporum* on Pecan in Brazil. Plant Dis 2020;104(6):1870. https://doi.org/10.1094/PDIS-09-19-1956-PDN.
[49] Mohamed RA, Al-Bedak OA, Hassan SH. First record in Upper Egypt of vascular wilt on pomegranate caused by *Fusarium oxysporum*, its molecular identification and artificial pathogenicity. J Plant Dis Prot 2021;128:311–6. https://doi.org/10.1007/s41348-020-00385-z.
[50] Al-Huqail AA, Hatata MM, Al-Huqail AA, et al. Preparation, characterization of silver phyto nanoparticles and their impact on growth potential of *Lupinus termis* L. seedlings. Saudi J Biol Sci 2018;25(2):313–9. https://doi.org/10.1016/j.sjbs.2017.08.013. PMid: 29472784.
[51] Janaki AC, Sailatha E, Gunasekaran S. Synthesis, characteristics and antimicrobial activity of ZnO nanoparticles. Spectrochim Acta A Mol Biomol Spectrosc 2015;144:17–22. https://doi.org/10.1016/j.saa.2015.02.041. PMid: 25748589.
[52] Shaikh S, Nazam N, Rizvi SMD, et al. Mechanistic insights into the antimicrobial actions of metallic nanoparticles and their implications for multidrug resistance. Int J Mol Sci 2019;20(10):2468. https://doi.org/10.3390/ijms20102468. PMid: 31109079.
[53] Jo Y-K, Kim BH, Jung G. Antifungal activity of silver ions and nanoparticles on phytopathogenic fungi. Plant Dis 2009;93(10):1037–43. https://doi.org/10.1094/PDIS-93-10-1037. PMid: 30754381.
[54] Kim SW, Jung JH, Lamsal K, et al. Antifungal effects of silver nanoparticles (AgNPs) against various plant pathogenic fungi. Mycobiology 2012;40(1):53–8. https://doi.org/10.5941/MYCO.2012.40.1.053. PMid: 22783135.
[55] Mishra S, Singh BR, Naqvi AH, et al. Potential of biosynthesized silver nanoparticles using *Stenotrophomonas* sp. BHU-S7 (MTCC 5978) for management of soil-borne and foliar phytopathogens. Sci Rep 2017;7(1):45154. https://doi.org/10.1038/srep45154. PMid: 28345581.
[56] Ferreira FV, Herrmann-Andrade AM, Calabrese CD, et al. Effectiveness of *Trichoderma* strains isolated from the rhizosphere of citrus tree to control *Alternaria alternata*, *Colletotrichum gloeosporioides* and *Penicillium digitatum* A21 resistant to pyrimethanil in post-harvest oranges (*Citrus sinensis* L. (Osbeck)). J Appl Microbiol 2020;129(3):712–27. https://doi.org/10.1111/jam.14657. PMid: 32249987.
[57] Gomaa A, Mahdy A, Fawzy R, et al. Control of tomato fusarium wilt caused by *Fusarium oxysporum* f. sp. *lycopersici* by grafting and silver nanoparticles under greenhouse conditions. Benha J Appl Sci 2022;7(5):37–50. https://doi.org/10.21608/bjas.2022.244584.
[58] Hwang ET, Lee JH, Chae YJ, et al. Analysis of the toxic mode of action of silver nanoparticles using stress-specific bioluminescent bacteria. Small 2008;4(6):746–50. https://doi.org/10.1002/smll.200700954. PMid: 18528852.
[59] Prabhu S, Poulose EK. Silver nanoparticles: Mechanism of antimicrobial action, synthesis, medical applications, and toxicity effects. Int Nano Lett 2012;2:32. https://doi.org/10.1186/2228-5326-2-32.
[60] Sondi I, Salopek-Sondi B. Silver nanoparticles as antimicrobial agent: A case study on *E. coli* as a model for Gram-negative bacteria. J Colloid Interface Sci 2004;275(1):177–82. https://doi.org/10.1016/j.jcis.2004.02.012. PMid: 15158396.
[61] Danilczuk M, Lund A, Sadlo J, et al. Conduction electron spin resonance of small silver particles. Spectrochim Acta A Mol Biomol Spectrosc 2006;63(1):189–91. https://doi.org/10.1016/j.saa.2005.05.002. PMid: 15978868.
[62] Kim JS, Kuk E, Yu KN, et al. Antimicrobial effects of silver nanoparticles. Nanomed Nanotechnol Biol Med 2007;3(1):95–101. https://doi.org/10.1016/j.nano.2006.12.001. PMid: 17379174.
[63] Feng QL, Wu J, Chen G-Q, et al. A mechanistic study of the antibacterial effect of silver ions on *Escherichia coli* and *Staphylococcus aureus*. J Biomed Mater Res 2000;52(4):662–8. https://doi.org/10.1002/1097-4636(20001215)52:4<662::AID-JBM10>3.0.CO;2-3. PMid: 11033548.
[64] Matsumura Y, Yoshikata K, Kunisaki S-I, et al. Mode of bactericidal action of silver zeolite and its comparison with that of silver nitrate. Appl Environ Microbiol 2003;69(7):4278–81. https://doi.org/10.1128/AEM.69.7.4278-4281.2003. PMid: 12839814.
[65] Morones JR, Elechiguerra JL, Camacho A, et al. The bactericidal effect of silver nanoparticles. Nanotechnology 2005;16(10):2346. https://doi.org/10.1088/0957-4484/16/10/059. PMid: 20818017.
[66] Hatchett DW, White HS. Electrochemistry of sulfur adlayers on the low-index faces of silver. J Phys Chem 1996;100(23):9854–9. https://doi.org/10.1021/jp953757z.
[67] Mashwani Z-U-R, Khan T, Khan MA, et al. Synthesis in plants and plant extracts of silver nanoparticles with potent antimicrobial properties: Current status and future prospects. Appl Microbiol Biotechnol 2015;99:9923–34. https://doi.org/10.1007/s00253-015-6987-1. PMid: 26392135.
[68] Mohanta YK, Biswas K, Jena SK, et al. Anti-biofilm and antibacterial activities of silver nanoparticles synthesized by the reducing activity of phytoconstituents present in the Indian medicinal plants. Front Microbiol 2020;11:1143. https://doi.org/10.3389/fmicb.2020.01143. PMid: 32655511.
[69] Sadak MS. Impact of silver nanoparticles on plant growth, some biochemical aspects, and yield of fenugreek plant (*Trigonella foenum-graecum*). Bull Natl Res Cent 2019;43(1):1–6. https://doi.org/10.1186/s42269-019-0077-y.
[70] Krishnaraj C, Jagan E, Ramachandran R, et al. Effect of biologically synthesized silver nanoparticles on *Bacopa monnieri* (Linn.) Wettst. plant growth metabolism. Process Biochem 2012;47(4):651–8. https://doi.org/10.1016/j.procbio.2012.01.006.
[71] Oh M-M, Trick HN, Rajashekar C. Secondary metabolism and antioxidants are involved in environmental adaptation and stress tolerance in lettuce. J Plant Physiol 2009;166(2):180–91. https://doi.org/10.1016/j.jplph.2008.04.015. PMid: 18562042.
[72] Abd-Ellatif S, Ibrahim AA, Safhi FA, et al. Green synthesized of *Thymus vulgaris* chitosan nanoparticles induce relative WRKY-genes expression in *Solanum lycopersicum* against *Fusarium solani*, the causal agent of root rot disease. Plants 2022;11(22):3129. https://doi.org/10.3390/plants11223129. PMid: 36432858.